Asian Journal of Chemistry; Vol. 23, No. 8 (2011), 3623-3625

ASIAN JOURNAL OF CHEMISTRY

www.asianjournalofchemistry.co.in

Ultrasound-Assisted Fast Synthesis of Mesoporous Silica Spheres with High Specific Surface Area

ZHIQIANG WANG, GUOSHENG HU*, JINGTING ZHANG and YINGCHUN LI

Shanxi Research Center of Engineering Technology for Engineering Plastics, North University of China, Taiyuan 030051, P.R. China

*Corresponding author: Fax: +86 351 3925158; Tel: +86 351 3925158; E-mail: huguosheng@nuc.edu.cn

(*Received*: 10 November 2010; *Accepted*: 27 April 2011) AJC-9861

A fast method for synthesis of mesoporous silica spheres was developed by using ultrasound as driving power, polyoxyethylene (20) sorbitan monolaurate as dispersant, tetraethoxysilane as silica source and octylamine as template. The as-prepared microspheres were characterized with field emitting scanning electron microscopy, thermogravimetry, X-ray diffraction and nitrogen (N_2) adsorption/desorption measurements, respectively. The experimental results showed that polyoxyethylene(20) sorbitan monolaurate could obviously decrease the size range of the products, which possessed specific surface area of 1272.6 m^2/g and narrow mesoporous distribution of about 0.5-2.5 nm. Moreover, the nanopores in the shell of mesoporous silica spheres became more and more unordered with the prolonging of the calcinating time.

Key Words: Mesoporous silica microspheres, Synthesis, Utrasonic wave, Tween 20.

INTRODUCTION

Recently, mesoporous silica spheres (MSS) with controlled morphology have received much attention and widely used in the fields of catalysis, adsorption, chromatography, controlled release of drugs and so on[1-5]. Up to now, some reaserchers had adopted 'spherical template' methods to control the structure of mesoporous silica spheres and the most frequently used ones were triblock copolymer[6], surfactant[7], polymer spheres[8], inorganic particles[9,10] and emulsions[11,12]. Although those products were desirable. The methods usually cost several hours to several days. However, in a modern world of materials science there is constant demand for saving time and simplifying synthetic methods.

In addition, ultrasonic method was regarded as one of the useful and efficient techniques for inducing chemical reaction and inhibiting particle agglomeration in aqueous solutions[13]. The main theory of this method is that ultrasound can create acoustic cavitation (formation, growth and implosion of bubbles) in a liquid. When cavitation bubbles collapse, small areas of high pressure differences are generated, resulting in micro turbulence and liquid jets. This create strong forces that act on the agglomerates, resulting in good dispersity[14]. Moreover, polyoxyethylene (20) sorbitan monolaurate (Tween 20) is a water-soluble non-ionic surfactant with low molecular weight[15] and the structural formula is shown as follows.

The surfactant possesses a branched hydrophilic region of three polyoxyethylene chains substituted to a sorbitan ring and is broadly used to lower the interfacial tension at oil-water interface and then to generate microsized products with desirable dispersity[16,17].

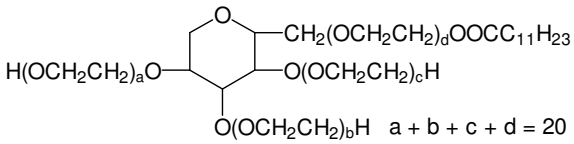

In this work, we have presented an efficient technology to synthesize mesoporous silica spheres with high specific surface area. The products were prepared by employing ultrasonic wave as driving power, Tween 20 as dispersant, tetraethoxysilane (TEOS) as silica source and octylamine (OA) as template and hydrolyst. The products were characterized by FE-SEM, TG, XRD and N_2 adsorption/desorption analysis, respectively.

EXPERIMENTAL

TEOS, Tween 20, OA were analytically pure and provided by Beijing Chemical Corporation.

Synthesis of mesoporous silica spheres: Typically, 4 mL OA, 10 mL TEOS and 1.5 mL Tween 20 were added in a 250 mL glass beaker at room temperature. The beaker was placed in an ordinary ultrasonic generator with the power of 100w (Model: JAC-100, China). 10 min later, 150 mL distilled water were added rapidly to the above solution. Then, the white samples were filtrated, repeatedly washed with alcohol for several times and dried in a drying closet at 70 ºC for 2 h.

Finally, the products were calcined in a muffle furnace at 650 ºC to remove the organic substances. The control mesoporous silica spheres samples were prepared without using Tween 20 *via* the same procedures.

Characterization: The morphology of the specimens was observed by Hatchi S-4800 field emitting scanning electron microscopy (FE-SEM). The thermal behavior was characterized by Netzsch STA449C thermogravimetry analysis (TG) in nitrogen atmosphere. The structural identification was characterized by Rigaku D/max small-angle (SXRD) and wide-angle X-ray diffraction (WXRD). The specific surface area and pore size distribution were carried out by a Quantachrome NOVA 2000 automated gas sorption instrument.

RESULTS AND DISCUSSION

Field emitting scanning electron microscopy analysis: Field emitting scanning electron microscopy images for control mesoporous silica spheres and mesoporous silica spheres are shown in Fig. 1. According to Fig. 1(a), as-prepared control mesoporous silica spheres possess relatively wide size range about 50-600 μm. However, mesoporous silica spheres [Fig. 1(b)] possess obviously narrow size range. The possible reasons about this result were that during the formation process of mesoporous silica spheres the size of OA vesicles were firstly decreased by the coordinating dispersal effects of ultrasound and Tween 20. Then, a fast hydrolysis and condensation of TEOS took place around OA vesicles and the morphology of the vesicles was fixed by a quick gelation process[18], resulting in organic-silica spheres. In addition, Tween 20 molecules could adsorb on the surface of mesoporous silica spheres to avoid agglomeration during the preparing, filtering and drying of mesoporous silica spheres and removed by calcinations.

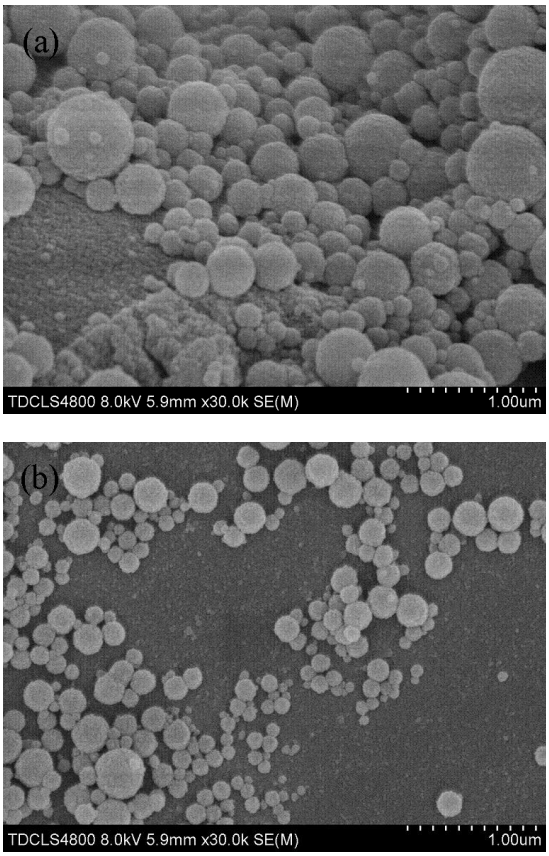

Fig. 1. FE-SEM images for (a) control mesoporous silica spheres and (b) mesoporous silica spheres

TG analysis: TG and TGA spectrums for mesoporous silica spheres are shown in Fig. 2. There are two endothermic peaks at 219.1 and 447.9 ºC, which are contributed by the decomposition of organic substances. The corresponding TG curve in Fig. 2(a) also clearly presents as two stages. One weight loss (15.8 %) occurs in the temperature range from 109.4-325.1 ºC. This is due to the combustion and carbonization of OA[19]. The second stage is from 325.1-649.1 ºC, a mass loss of about 23.1 % is observed, which can be assigned to the decomposition of Tween 20. Therefore, the optimal calcinating temperature was about 650 ºC.

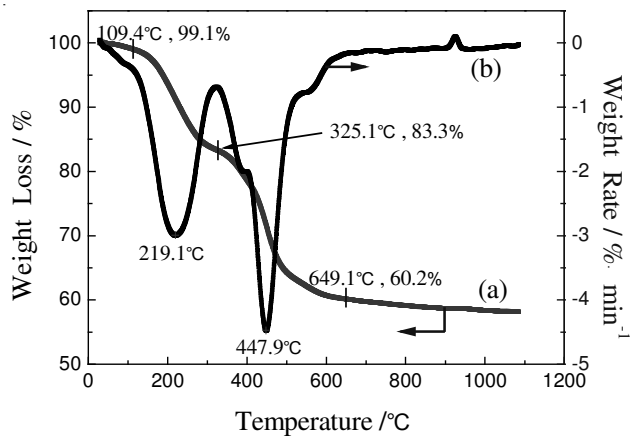

Fig. 2. TG (a) and TGA (b) spectrums for mesoporous silica spheres

X-Ray diffraction analysis: WXRD spectrum for mesoporous silica spheres calcined for 3 h and SXRD spectrums for mesoporous silica spheres calcined for 3, 12 and 36 h are shown in Fig. 3, respectively. It can be clearly seen that only one broad diffraction peak in WXRD specimen can be observed, illustrating that mesoporous silica spheres were amorphous structure. It can also be seen in the inset that a sharp diffraction peak at 2.4 of 2θ degree in Fig. 3(a). This result obviously demonstrates that mesoporous silica spheres calcined for 3 h are mesoporous materials[20] and the nanopores are regularly distributed in the shell[21]. However, mesoporous silica spheres calcined for 12 and 36 h exhibit patterns with no diffraction peak (Fig. 3(b) and (c)) and further illustrate that the nanopores become more and more unordered. The reasons about this change may be that the shell of mesoporous silica spheres becomes increasingly densefied as prolonging of the calcinating time.

Nitrogen adsorption/desorption analysis: Nitrogen-adsorption/desorption isotherm and corresponding pore-size distribution (inset) for mesoporous silica spheres are presented in Fig. 4. It can be seen that a type of IV curve with hysteresis is obviously observed, clearly demonstrating that mesoporous silica spheres are mesoporous structure[22], in addition, in Fig. 4 (inset), narrowly distributed nanopores width from about 0.5-2.5 nm and centered at 1.2 nm, is showed. Calculations indicate that the products have high specific surface area of 1272.6 m^2/g.

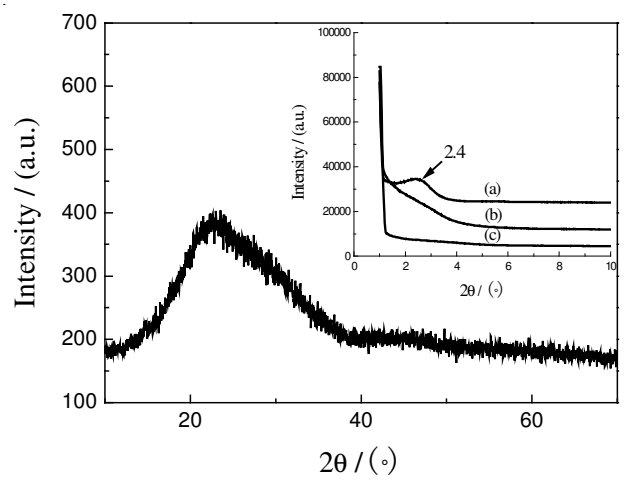

Fig. 3. WXRD spectrums for mesoporous silica spheres calcined for 3 h and the inset shows SXRD spectrums for mesoporous silica spheres calcined for different hours, (a): 3 h, (b): 12 h, (c): 36 h

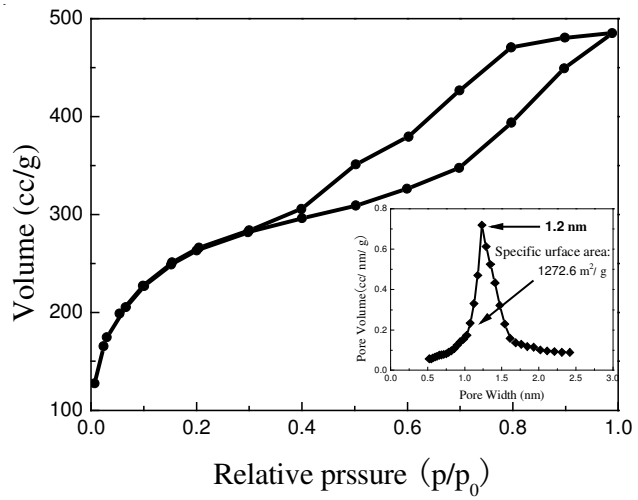

Fig. 4. N_2-adsorption/desorption isotherm and corresponding pore-size distribution (inset) for mesoporous silica spheres which were calcined for 3 h

Conclusion

In summary, mesoporous silica spheres with high specific surface area were synthesized by employing ultrasound as driving force, Tween 20 as dispersant, TEOS as silica source and OA as template. The experimental results showed that Tween 20 could decrease the size range of the products and the optimal calcinating temperature was about 650 ºC. Moreover, the nanopores in the shell of mesoporous silica spheres became more and more unordered with the prolonging of the calcinating time.

ACKNOWLEDGEMENTS

The authors gratefully acknowledged the financial support of National Natural Science Foundation of China (No. 20571066).

REFERENCES

1. M.E. Davis, *Nature*, **417**, 813 (2002).
2. A. Stein, *Adv. Mater*., **15**, 763 (2003).
3. X.L. Yu, S.J. Ding, Z.K. Meng, J.G. Liu, X.Z. Qu, Y.F. Lu and Z.Z. Yang, *Colloid. Polym. Sci*., **286**, 1361 (2008).
4. C. Chen, S. Cheng and L.Y. Jang, *Micropor. Mesopor. Mater*., **109**, 258 (2008).
5. X.F. Wu, H.R. Lu, Z.Q. Wang and X.H. Xu, *J. Sol-Gel Sci. Technol*., **54**, 147 (2010).
6. Y. Chen, Y.J. Wang, L.A.Yang and G.S. Lu, *AlChe. J.*, **54**, 298 (2008).
7. Y.F. Zhu, J.L. Shi1, W.H. Shen, H.R. Chen, X.P. Dong and M.L. Ruan, *Nanotechnology*, **16**, 2633 (2005).
8. M. Yang, G. Wang and Z.Z. Yang, *Mater. Chem. Phys*., **111**, 5 (2008).
9. Y. Le, J.F. Chen, J.X. Wang, L. Shao and W.C. Wang, *Mater. Lett*., **58**, 2105 (2004).
10. J.F. Chen, H.M. Ding, J.X. Wang and L. Shao, *Biomaterials*, **25**, 723 (2004).
11 J.B. Miao, J.S. Qian, X.H. Wang, Y.C. Zhang, H.Y. Yang and P.S. He, *Mater. Lett*., **63**, 989 (2009).
12. B. Tan and S.E. Rankin, *Langmuir*, **21**, 8180 (2005).
13. H.X. Li, H. Li, J. Zhang, W.L. Dai and M.H. Qiao, *J. Catal*., **246**, 301 (2007).
14. C. Sauter, M.A. Emin, H.P. Schuchmann and S. Tavman, *Ultrason. Sonochem*., **15**, 517 (2008).
15. S. Kerstens, B.S. Murray and E. Dickinson, *J. Colloid Interf. Sci*., **296**, 332 (2006).
16. J.L. Henry, P.J. Fryer, W.J. Frith and I.T. Norton, *J. Colloid Interf. Sci*., **338**, 201 (2009).
17. L. Yobas, S. Martens, W.L. Ong and N. Ranganathan, *Lab. Chip*., **6**, 1073 (2006).
18. K. Kosuge, T. Murakami, N. Kikukawa and M. Takemori, *Chem. Mater*., **15**, 3184 (2003).
19. X. Tang, Z. Su, Y. Han and Z.H. Liu, *Colloid Surf. A*, , **317**, 443 (2008).
20. S.A. Bagshaw, E. Prouzet and T.J. Pinnavaia, *Science*, **269**, 1242 (1995).
21. S.Q. Liu, J.C. Rao and X.Y. Sui, *J. Non-Cryst. Solids*, **354**, 826 (2008).
22. X.L. Ji, Q.Y. Hu, J.E. Hampsey, X.P. Qiu, L.X. Gao, J.B. He and Y.F. Lu, *Chem. Mater*., **18**, 2265 (2006).